

Colloid Facilitated Migration of Radioelements - Mechanisms, Significance, and Needed Conditions

JOHN M. ZACHARA¹, MARKUS FLURY², AND JAMES HARSH²

¹Pacific Northwest National Laboratory, Richland, WA

²Washington State University, Pullman, WA

Colloids are fine-grained particulates (1 nm – 1 μm) present in near surface geologic materials. They result from i.) the degradation of organic detritus, ii.) mineral weathering, and iii.) various in-situ precipitation reactions. Colloidal materials enhance the sorption capacity of the solid phase when aggregated or bound to the surfaces of larger, immobile particles because their high surface area, electrostatic properties, and surface functional groups favor inorganic solute complexation. Under aqueous conditions that promote their dispersion and stability, colloidal material can facilitate the migration of radioelements that strongly sorb to them leading to more widespread dispersal. Here we describe accounts of colloid facilitated radioelement migration, generalizing controlling factors such as colloid identity and concentration; aqueous phase conditions; and contaminant sorption mechanism, strength, and reversibility. Then, the subsurface migration of ¹³⁷Cs will be evaluated in a high-level nuclear waste vadose zone plume at the Hanford site where alkaline, high-ionic strength ¹³⁷Cs –containing solutions have migrated 30 m through the subsurface, yielding an anomalous distribution profile. ¹³⁷Cs⁺ is a strongly sorbing cation whose migration is facilitated by high Na⁺ in the waste-water. Low ionic strength meteoric waters currently infiltrate the site that dilute pore-water Na⁺ and increase adsorptive affinity and colloid migration potential. Laboratory experiments documented the occurrence of waste-induced mineral dissolution and precipitation reactions leading to the formation of fine-grained zeolitic phases including sodalite and cancrinite. These phases have comparable ¹³⁷Cs adsorptivity to the indigenous sediment sorbents (phyllosilicates) and exhibit surface charge characteristics conducive to particle migration. Column studies were performed with pristine and contaminated sediments that demonstrate the potential for colloid migration of a portion of the adsorbed ¹³⁷Cs pool. The implications of colloid migration to the existing contaminant plume and future migration are discussed.

Evidence for Li isotope fractionation during subduction

T. ZACK¹, P.B. TOMASCAK², W.F. McDONOUGH², R.L. RUDNICK², AND C. DALPE²,

¹ Mineralogisches Institut, Universität Heidelberg, Im Neuenheimer Feld 236, 69120 Heidelberg, Germany

²Geology Department, University of Maryland, College Park, MD 20740, USA

Compared to the mantle, subducted oceanic crust is generally heavy in Li isotope composition, potentially making Li isotopes a powerful tracer for the subduction component in island arcs. However, preliminary data (Zack et al., 2001; Goldschmidt 2001) has shown that subducted basalts (orogenic eclogites from Trescolmen, Switzerland) can be isotopically very light. The two lightest eclogites have $\delta^7\text{Li}$ values of -8.5‰ and -9.6‰, with replicates of both samples being within the established analytical 2σ uncertainty of 1‰. Mechanisms that can be ruled out as producing such light compositions (Zack et al., submission to EPSL) include:

(1) High-T alteration. One amphibolite-facies ocean floor basalt measured by Chan et al. (1992; EPSL 108: 151-160) is light in terms of $\delta^7\text{Li}$. However, Trescolmen eclogites have chemical patterns characteristic of low-T altered basalts, e.g. $\delta^{18}\text{O}$ up to +7.5‰ (Wiesli et al., 2001; Int. Geol. Rev. 43: 95-119) and elevated Na and LILE concentrations.

(2) Fluid influx from surrounding garnet mica schists. Although there is widespread evidence for fluid exchange between eclogites and adjacent metapelites at high P conditions, this process can have only elevated $\delta^7\text{Li}$, as the mica schists have consistently heavier $\delta^7\text{Li}$ (+2.4 to +3.8‰).

(3) Amphibolite-facies overprint. Eclogites show variable, although minor, signs of retrogression due to hydration by an amphibolite-facies fluid influx. Such retrogressed areas can be excluded by analysing carefully selected pure omphacite mineral separates, as omphacite contains most of the Li in eclogites. The $\delta^7\text{Li}$ of eclogite whole rocks overlaps with that of corresponding omphacite separates within analytical uncertainty, demonstrating that post-eclogite-facies retrogression has not changed the Li isotope composition significantly.

We suggest that the very light $\delta^7\text{Li}$ values (down to -9.6‰) in the eclogites is produced by isotopic fractionation during early devolatilization of low-T altered basalts. Here, fluid loss by Rayleigh distillation between 100-300°C efficiently releases heavy Li to the fluid while the residue is subsequently depleted in ⁷Li. These data support previous suggestions that isotopically heavy Li is released into the forearc mantle wedge in subduction zones, while isotopically light Li is subducted deeply, forming a distinct mantle reservoir.

Computer Simulation of Uranyl Adsorption on Montmorillonite Clay

O. F. ZAIDAN¹, J. A. GREATHOUSE¹, AND
R. T. PABALAN²

¹Dept. of Chemistry, St. Lawrence University, Canton, New York, USA (jgreathouse@stlawu.edu)

²Center for Nuclear Waste Regulatory Analyses, Southwest Research Institute, San Antonio, Texas, USA (rpabalan@swri.edu)

Introduction and Methods

We performed computer simulations to study the adsorption characteristics of the aqueous uranyl ion (UO_2^{2+}) near the siloxane surface of montmorillonite, a smectite clay. Our goal is to better understand the fate of uranium waste products in groundwater and soil sediments, a problem of increasing importance in environmental geochemistry.

We used the Monte Carlo simulation methodology and clay potential parameters of Skipper et al. (1995). Potential parameters for the aqueous uranyl ion yield a coordination geometry consistent with experimental data (Gilbaud et al., 1996). In our simulations, we have investigated the clay $d(001)$ spacing and uranyl coordination structure as a function of water content. The simulation supercell consisted of approximately 8 unit cells of the mineral, 3 UO_2^{2+} ions, and N interlayer water molecules.

Results

We examined the interlayer structure as the water content (N) was increased from 0 (dry clay) to 96 (300 mg $\text{H}_2\text{O}/\text{g}$ clay). The table below shows layer spacing and average U–O and U–Si distances (obtained from radial distribution functions). The uranyl ions are oriented with the O–U–O axis tilted slightly from the surface normal. Even at low water content ($N = 30$), the U–Si distance indicates that the uranyl ions do not form inner-sphere surface complexes. The first U–O peak at 2.45 Å is comprised exclusively of water oxygen atoms with a coordination number of 5. The second broader peak at 4.25 Å is due to both water and surface oxygen atoms. Two distinct water layers are seen at $N = 60$, with a $d(001)$ spacing of 14.72 Å. This layer spacing agrees well with the experimental value of 14.81 Å (Giaquinta et al., 1997).

N	$d(001) / \text{Å}$	U–O dist. / Å	U–Si dist. / Å
0	11.45 ± 0.07	2.60, 4.95	3.10
30	13.15 ± 0.14	2.45, 4.25	4.80
60	14.72 ± 0.09	2.45, 4.35	4.95
90	16.87 ± 0.13	2.45, 4.70	4.85

References

- Giaquinta D.M., Soderholm L., Yuchs S.E. and Wasserman S.R., (1997), *Radiochim. Acta* **76**, 113-121.
 Gilbaud P. and Wipff G., (1996), *J. Mol. Struct.* **366**, 55-63.
 Skipper N.T., Chang F.-R.C. and Sposito G., (1995), *Clays Clay Miner.* **43**, 285-293.

Carbon and oxygen isotope compositions of carbonatite complexes from the Kola Peninsula, Russia

A.N. ZAITSEV¹, A. DEMÉNY², F. WALL³, S. SINDERN⁴,
M.A. SITNIKOVA¹, P.I. KARCHEVSKY¹

¹ St Petersburg State University, 7/9 University Emb., 199034 St Petersburg, Russia; (anatolz@hotmail.com)

² Laboratory for Geochemical Research, Hungarian Academy of Sciences, Budaorsi ut 45, 1112 Budapest Hungary; (demeny@geochem.hu)

³ Natural History Museum, Cromwell Road, London, SW7 5BD, UK.

⁴ RWTH-Aachen, Wullnerstr. 2, 52056 Aachen, Germany

The Kola-Karelia Region of Russia and Finland contains many carbonatite complexes, most of which are part of the Palaeozoic Kola Alkaline Province. Stable carbon and oxygen isotope compositions from published data (Khibina et al.) and new data (Sallanlatvi et al.) are compared here in order to find general patterns in the nature of their mantle source. The samples investigated contain several carbonate minerals and also several stages of carbonatite crystallization in order to have a complete view on carbonatite genesis and evolution.

Original (mantle) compositions are often modified in carbonatites by processes of fractional crystallization, degassing, and hydrothermal alteration. Careful consideration has been given to eliminating these processes before comparing the remaining primary compositions. For example, a recent study of REE-rich carbonatites at Khibina and Vuorijarvi, involving a combination of detailed mineral chemical investigation, stable (C,O) and radiogenic (Sr, Nd) isotopes, showed that each has a pegmatitic stage where a REE mineral (burbankite) and calcite or dolomite are co-genetic. Subsequent alteration caused much wider variation in stable isotopic values.

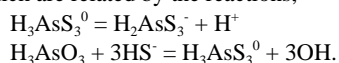
The primary oxygen isotope compositions are uniform (7 to 8 ‰) but there are large variations in $\delta^{13}\text{C}$ from normal mantle compositions (~ -6 ‰) to rather high $\delta^{13}\text{C}$ values (~ -2 ‰) which are independent of the age of the complex. The data are best explained by mantle heterogeneity caused by CO_2 metasomatism. In the Khibina and Vuorijarvi REE-rich carbonatites which are very similar as described above, the $\delta^{13}\text{C}$ ranges of primary carbonatites with low (unaltered) $\delta^{18}\text{O}$ values are different from each other but are correlated with their radiogenic isotope compositions. Interestingly, the Khibina complex with normal mantle $\delta^{13}\text{C}$ values have higher Sr isotope ratios than the Vuorijarvi carbonatites with relatively high $\delta^{13}\text{C}$. This difference is even more pronounced if other complexes (e.g. Kovdor and Turij) are also included in the comparison. The relationship between $\delta^{13}\text{C}$ and radiogenic isotope compositions is opposite to what would be expected in case of mantle contamination by subducted sedimentary carbonate. The data appear best explained by subduction-related source contamination facilitated by CO_2 metasomatism that caused $\delta^{13}\text{C}$ variations in the different mantle components.

Spectrophotometric study of thioarsenite speciation in high temperature aqueous solutions

V.P.ZAKAZNOVA-IAKOVLEVA AND T.M. SEWARD

Institut für Mineralogy und Petrographie, ETH-Zentrum,
CH-8092, Zürich, Switzerland

Arsenic sulphides occur commonly in natural waters, especially in hydrothermal systems. For example, in the Rotokawa geothermal system in New Zealand bright yellow and orange precipitations of amorphous arsenic sulphides are observed around near-boiling springs. In addition, the deep fluids have arsenic concentrations up to 3-4 ppm (Krupp and Seward, 1990). The lower temperature hydrothermal chemistry of arsenic also has some relevance to understanding the metabolic processing of arsenic by thermophiles in the near surface environment of hydrothermal systems. Unfortunately, thioarsenite speciation in aqueous solutions is not well determined; there is no agreement in the literature, although there are experimental solubility data, Raman spectroscopic measurements, and theoretical calculations in As-S-H₂O aqueous system. The present study involves the determination of the stabilities and stoichiometry of thioarsenous species in aqueous solutions from 25 to 300°C by means of high temperature uv-vis spectrophotometry. Absorbance measurements were carried out in a flow-through Ti-Pd alloy cell with windows of uv-quality fused silica. Spectra were collected using a Cary 5E double beam spectrophotometer. Solution preparation and handling as well as pH determination were carried out in such a way as to exclude any contact with air and in some cases also without any gaseous phase to avoid losses of H₂S. Rank analysis of the absorbance matrix indicated the presence of the three species in solution, one of which could be ascribed to the HS⁻ ion charge-transfer-to-solvent transition. The other two absorbing species we ascribed to be H₃AsS₃⁰ and H₂AsS₃⁻, which are related by the reactions,



References

Krupp R. E. and Seward T. M., (1990), *Mineral. Depos.* **25**, 73-81.

The relationship between volatile element patterns and chondrule textures in CRs and OCs

B. ZANDA^{1,2}, M. HUMAYUN³, R. H. HEWINS²,
M. BOUROT-DENISE¹ AND A. J. CAMPBELL³

¹CNRS/Minéralogie MNHN, 75005 Paris, France.

²Geological Sciences, Rutgers University, Piscataway, NJ 08855, USA, (zandahew@rci.rutgers.edu)

³Geophysical Sciences, University of Chicago, Chicago, IL 60637, USA.

The chemical complementarity between chondrules and matrix has been considered to show that they represent material condensed at different temperatures¹. The nature of the chemical complementarity is, however, different between different meteorites, e.g. Renazzo and Semarkona, and here we show that chemical differences correspond to textural differences that yield insight into the nature and environment of chondrule formation.

Volatile-depleted CR chondrites preserve evidence of extensive volatilization during chondrule formation rapidly followed by incomplete recondensation, onto chondrule rims for moderately volatile elements and in the matrix for the most volatile elements such as S, Ga, Ge etc². The matrix represents a large fraction of CR [31.1% in Renazzo] chondrites and CR chondrules are often irregular in shape and preserve evidence of formation by the agglomeration of smaller droplets in a dust-rich environment.

Ordinary chondrites on the other hand, are less volatile-depleted and contain less matrix [15.6% in Semarkona]. In contrast to CRs, a large fraction of the chondrules are volatile-enriched and volatile elements such as S are concentrated in veneers around chondrules. This indicates that recondensation after chondrule formation was dominantly onto chondrules rather than in the sparse matrix. OC chondrules are typically spherical, but also preserve evidence for having agglomerated together and with their surrounding matrix at temperatures above the glass transition temperature, as they are frequently molded around one another.

We interpret this as evidence that (i) matrix must have been present in the same nebular region as the chondrules when these were still hot, (ii) the first stages of accretion followed chondrule formation rapidly enough that the matrix-chondrule system remained closed, (iii) chondrules had cooled down to lower temperatures in OCs than in CRs when this event took place, which allowed a more complete recondensation. This argues against the x-wind model³ for chondrule formation, according to which volatiles lost from chondrules ought to be decoupled from them. It is consistent, however with the predictions of the shock-wave model⁴.

References

¹Palme H. and Klerner S. (2000), *MAPS* **35**, A124.

²Campbell A., Humayun M. and Zanda B. (2002) *this conf.*

³Shu F. H. et al. (1997), *Science* **277**, 1475-1479.

⁴Desch S. and Connolly H. C. Jr (2002), *MAPS* **37**, 183-207.

Annite: magmatic evolution and subsolidus alteration in nepheline syenites, Mount Saint-Hilaire, Quebec, Canada

AZIN ZANGOUI

Earth & Planetary Sciences, McGill University, 3450
University St., Montreal, Quebec, Canada H3A 2A7
(azin@eps.mcgill.ca)

Mount Saint-Hilaire (MSH) forms part of the Monteregian alkaline SiO₂-undersaturated intrusions, first grouped and described by Hunt (1859). At MSH, the East Hill suite (Currie *et al.* 1983), is well exposed in the Poudrette quarry, where the samples were collected for this research. Nepheline syenite represents the most highly differentiated product of igneous activity at MSH. It also records a significant subsolidus overprint due to circulation of post-magmatic fluids. Annite forms about 20% of the typical nepheline syenites, and can be a sensitive monitor of magmatic phenomena and of post-magmatic alteration. Annite has been analysed from porphyritic nepheline syenite, poikilitic nepheline syenite, Poudrette dyke (nepheline syenite pegmatite), sodalite syenite, and completely altered nepheline syenite by means of electron-microprobe to document the evolution of annite in terms of composition and its textural development. Altered nepheline syenites are also characterized by transmission electron microscopy and XRD to elucidate the modification of the layers as well as the existence of micro-inclusions along the cleavage planes of annite. Although crystallization sequence of porphyritic and poikilitic syenites are markedly different, and reflect kinetic effects in addition to compositional factors, annite crystallizes in later stages of solidification of poikilitic nepheline syenites. The most recent map of the Poudrette quarry has been done by the author.

References

- Currie K. L., 1983. An interim report on the geology and petrology of the Mont Saint-Hilaire pluton, Quebec. Geological Survey of Canada Bulletin, 83-1B: 39-46
Hunt, T.S. 1859. Report for the year 1858. In Geological Survey of Canada, Report of progress for the Year 1858, pp.177-188

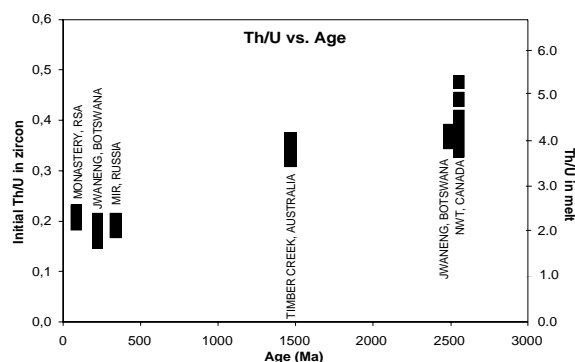
Evidence from kimberlitic zircon for a decreasing mantle Th/U

R. E. ZARTMAN AND S. H. RICHARDSON

Department of Geological Sciences, Univ. of Cape Town,
Rondebosch 7700, South Africa (rzart@yahoo.com)

A decoupling in MORB of measured Th/U ($\kappa=2.7$) from that calculated by Pb isotopes ($\kappa=3.8$) for the depleted asthenosphere is well established, and has been referred to as the second Pb paradox [1] or the kappa conundrum [2]. More controversial has been the cause and timing of this phenomenon, although the recycling of crustal Pb together with a higher return flux of U⁺⁶ relative to Th⁺⁴ into the mantle offers a plausible explanation. Such a mechanism operating over the past 2.5 Ga was modelled in Plumbotectonics [3], and found to be quantitatively feasible.

A large TIMS, ICP-MS, and IMP database of Th and U concentrations for kimberlite-hosted zircon, particularly from Cr-poor megacrystic suites, now exists [4-8]. Six suites comprised of 10 or more zircon reveal consistent patterns when plotted on Th/U vs. U diagrams. We interpret these patterns as resulting from fractional crystallization of a kimberlite-related fluid, permitting the extrapolation to an initial Th/U at the time zircon crystallization began. [Omitted are zircons, especially with high U contents, that appears not related to simple fractionation but may be of metasomatic origin.] A consistent decrease occurs in the zircon's initial Th/U over the past 2.5 Ga (see figure), suggesting that a similar change has occurred in the coexisting fluid. Estimates of Th and U distribution coefficients between zircon and melt permit calculation of Th/U in the melt, which, for these highly incompatible elements, should be the same as for its mantle source rock. Thus, kimberlitic zircon may indeed record a ~x2 reduction in κ since the Archean for the depleted asthenosphere.



References

- [1] Kramers J.D. and Tolstikhin I.N. (1997) *Chem. Geol.* **139**, 75-110. [2] Elliot T., Zindler A. and Bourdon B. (1999) *EPSL* **169**, 129-145. [3] Zartman R.E. and Haines S. (1988) *GCA* **52** 1327-1339. [4] Griffin et al. (2000) *GCA* **64** 133-147. [5] Kinny et al. (1989) *Geol. Soc. Aust. Spec. Publ.* **146**, 833-842. [6] Berryman et al. (1999). [7] Setsu et al. (2002) *EPSL* **175** 1-16. [8] Unpublished UCT data.

A comparison of carbon isotope composition and impurity defects of microdiamonds of octahedral and cubic habit from Udachnaya kimberlite pipe (Yakutia)

ZEDGENIZOV D.A., REUTSKY V.N., SHATSKY V.S., FEDOROVA E.N.

Institute of Mineralogy and Petrography, Pr. ak. Koptuyuga 3, Novosibirsk, 630090, Russia, e-mail: zed@uiggm.nsc.ru

According to present concepts, growth forms for diamonds are an octahedron at the layer-by-layer mechanism and a cuboid at the adhesive one. Hence we have carried out a comparative study of microdiamonds of octahedral and cubic habit from Udachnaya kimberlite pipe.

As on our and previously published data [Kinny et al., 1999], isotopic composition of carbon for microdiamonds of octahedral habit from Udachnaya pipe is from -0,85 to -7,16 ‰ (δ^{13}_{-mean} : -4,57 ‰; σ =1,54; n=18). Microdiamonds of cubic habit have a range of δ^{13}_{-} from -2,02 to -6,14 ‰ (δ^{13}_{-mean} - 4,46 ‰; σ =1,02; n=24).

Predominant nitrogen defects in microdiamonds of octahedral habit are IaA and IaB. The total nitrogen content in these crystals are mainly no more 350 ppm. At that about 50% of octahedra are nitrogen-free according to IR data (II_ type). The degree of nitrogen aggregation (IaB/IaA ratio) for octahedral crystals is more than 50%. Microdiamonds of cubic habit are characterized by presence of nitrogen only as IaA. The nitrogen content in cuboids (750-3000 ppm) is much higher than in studied octahedra. Complementary characteristic of all cuboids is the presence of hydrogen peaks in IR spectra.

On the diagram δ^{13}_{-}/N [Cartigny et al., 2001] studied microdiamonds make up two non-overlapping fields. The upper field is formed by microdiamonds of cubic habit and lower – by octahedral microcrystals. The coincidence of carbon isotope composition of two different microdiamond populations suggests the absence of correlation of growth mechanism and isotopic composition of carbon for diamonds. Nevertheless obtained results reveal the influence of diamond growth mechanism on the content of nitrogen impurity. Adhesive growth mechanism favor to capture of impurities, whereas layer-by-layer one provide for growth of diamonds with low nitrogen content. Similar situation was previously described by us for “re-shaped” microdiamonds, where the change of growth mechanisms are found [Zedgenizov et al.].

This work was supported by INTAS (YSF 00-197) and Russian Science Support Foundation.

References

- Kinny P.D., Trautman R.L., Griffin B.J., Harte B. (1999) Proceedings of the 7 Int. Kimb. Conf., v.1, pp.429-436.
 Cartigny P.; Harris J.W.; Javoy M. (2001) EPSL, v.185, Iss.1-2, pp.85-98.
 Zedgenizov D.A., Shatsky V.S., Politov A.A., Rylov G.M. Eur.J.Mineral., (under review).

Characterization of Microscale Flow through Porous Media During Geologic Sequestration of CO₂

BINIAM ZERAI¹, JAIKRISHNAN KADAMBI², BEVERLY SAYLOR¹

¹Department of Geological Sciences, Case Western Reserve University, Cleveland, OH 44106-7216 USA (bxz11@po.cwru.edu)

²Department of Aerospace and Mechanical Engineering, Case Western Reserve University, Cleveland, OH 44106-7216 USA (jxk11@po.cwru.edu)

We are developing a technique using Particle Image Velocimetry (PIV) to map microscale porous fluid flow. Our motivation is to understand the mixing of brine and CO₂ during aquifer sequestration of CO₂ and its impact on mineral-brine-CO₂ reactions. However, the dynamics of microscale fluid flow through pores and pore throats has applications to a variety of small-scale geochemical processes that take place in aquifers, soils, and other porous geological formations. For example, the pore-scale flow path through a heterogeneous rock or soil determines which minerals come into contact with fluid and the reactive surface area. Changes in flow velocity, such as at the mouth of a pore, may account for such phenomena as blocking of the downstream side of a pore throat by mineral precipitates.

PIV is a non-intrusive imaging technique for characterising multiphase flows. It requires an optically transparent test section, and refractive index matching of the test section and test fluid. The fluid is seeded with particles selected to have near neutral buoyancy and refractive index higher than that of the test section. The particles follow the flow and their path is imaged by periodic illumination by a sheet of laser light. The displacement of particles between illumination events is converted into velocity vectors.

We have constructed a clear plastic 2-D diagonal network model consisting of cylindrical pores, 2.5 mm across and 1.4 mm deep, connected by diagonal pore throats, 2.5 mm long across 1.4 mm deep. Pore throat widths vary randomly between 0.2 mm and 1.4 mm. NaI solution is seeded with 2 micron silicon carbide particles. This experimental design allows us to study the interface between 2 fluids at the scale of the test section and, using micro PIV, to map the fluid flow and interface within a single pore or pore throat.

Geochemistry of Proterozoic basic-ultrabasic volcanics from the west of Yangtze Plate: Implications for the crust-mantle evolution

H. X. ZHANG¹, Z. F. XU¹ AND C. -Q. LIU²

¹The institute of Geology and Geophysics, Chinese Academy of Sciences, Beijing, China (hxzhang@cashq.ac.cn)

²The institute of Geochemistry, Chinese Academy of Sciences, Guiyang, China (liucq@mimi.cnc.ac.cn)

Introduction

Many Proterozoic intraplate basic-ultra basic rocks were found in the west of Yangtze Plate, which can provide important information on Proterozoic crust-mantle evolution. Proterozoic within-plate basic-ultra basic volcanic rocks have been studied for their trace element and isotopic compositions in order to understand mantle geochemistry and crust-mantle evolution.

Discussion and Conclusion

Palaoproterozoic mafic volcanics pose EMI features and are thought to be formed in island arc-back arc setting related to the plate subduction of pre-Tethys Proterozoic Ocean Plate beneath paleo-Yangtze Plate. Geochemistry of the middle Proterozoic Caiziyuan peridotites shows that the formation of the peridotites is associated with the epicontinental basin at the ocean-land boundary or intracontinental rift basins. These observations suggest that the mantle source could have been metasomatized by the subduction-related dehydration fluids. In response to the Palaoproterozoic subduction, Neoproterozoic epicontinental or intracontinental rifts were formed, accompanied by formation of intra-plate hot-spot Dahongshan diabase. Whole-rock Sm-Nd isochron age of 1066 ± 110 Ma was obtained for the diabase. The enrichments of incompatible elements and radiogenic Nd isotope of the diabase suggest that their mantle source could have been affected by the primary volatile from asthenosphere and mantle plume.

Carbon cycling in the Gulf of Mexico gas hydrate systems: A review

¹C. L. ZHANG, ²R. SASSEN, AND ³B. LANOIL

¹Dept. Geol. Sci., Univ. Missouri-Columbia, MO 65 211, USA (zhangcl@missouri.edu)

²GERG, Texas A&M Univ., College Station, TX 77843, USA (sassen@gerg.tamu.edu)

³Dept. Environ. Sci., Univ. California, Riverside, CA 92521, USA (brian.lanoil@ucr.edu)

The Gulf of Mexico has abundant gas hydrates and hydrocarbon seeps. Geochemical evidence indicates that anaerobic oxidation of hydrocarbons, including methane, plays an important role in carbon cycling and the development of biological communities in gas hydrate systems. The following summarizes our current knowledge and understanding of anaerobic hydrocarbon oxidation in the Gulf of Mexico.

1. Lipid biomarkers and stable carbon isotopes suggest that anaerobic methane oxidation is mediated by consortia of sulfate-reducing bacteria and Archaea.

2. 16S rDNA indicate the presence of diverse bacterial species including sulfate-reducing bacteria and a limited diversity of Archaea, all of which are related to methanogens.

3. As a result of anaerobic hydrocarbon oxidation, large amounts of ¹³C-depleted carbonates precipitate on the bottom of ocean floor, which provide a favorable surface for the establishment of chemosynthetic communities in the deep sea.

4. Abundance of archaeal biomarkers and stable isotope signatures are similar to those of the Mediterranean mud volcanoes but are distinct from those of the Hydrate Ridge or Cascadia Ridge, suggesting variation in microbial communities or methane oxidation kinetics associated with different geological settings.

5. Anaerobic oxidation of oil hydrocarbons (>C₁₅) also occurs in the Gulf of Mexico, which has not been well studied, but may contribute significantly to carbon cycling in the Gulf of Mexico.

Our future research is focused on identification of microbial species and quantification of the processes of hydrocarbon oxidation, which link closely to macrofauna ecology. We will also develop conceptual models of carbon cycling coupled to other geochemical reactions in the Gulf of Mexico. Such studies should enhance our understanding of microbial biocomplexity in the deep-sea ecosystem and may shed light on the microbial evolutionary pathways in cold, hydrocarbon-rich extreme environments.

Acknowledgments: We would like to thank the following people (in alphabetic order), who contributed to this study: D. R. Cole, C. Fisher, J. Horita, Y. Huang, L. Larsen, Y. Li, T. Lyons, R. Pancost, A. Peacock, Y. Qian, J. Wall, Y. Wang, and D. C. White. This research is supported by National Science Foundation, USA.

$^{87}\text{Sr}/^{86}\text{Sr}$ of apatites from Altay No.3 pegmatite and its implications

H. ZHANG AND C.-Q. LIU

Lab. for Study of the Earth's Interior and Geofluids, IGCAS,
P.R. China (zhanghui65@hotmail.com)

Introduction: Up to now, there still exists a controversy if $^{87}\text{Sr}/^{86}\text{Sr}$ ratios in apatites have been perturbed in the alteration process. The purpose of this study is to reveal the variations of Sr isotope in pegmatitic system and its mechanism.

Discussion of the results: The apatites in this study yield high and variable $^{87}\text{Sr}/^{86}\text{Sr}$ ratios between 0.7922 and 1.2112. Fig.1 shows that the $^{87}\text{Sr}/^{86}\text{Sr}$ ratios of apatites scatter and have no correlation with their $^{87}\text{Rb}/^{86}\text{Sr}$ ratios, and data mainly distribute in three regions.

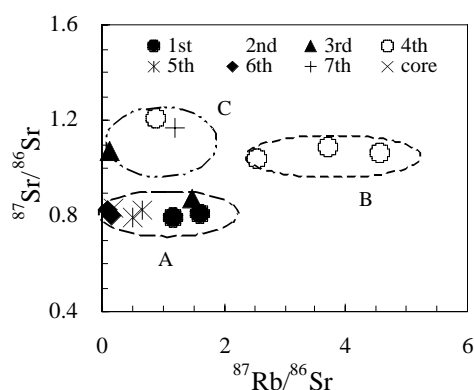


Fig.1. Plot of $^{87}\text{Sr}/^{86}\text{Sr}$ vs. $^{87}\text{Rb}/^{86}\text{Sr}$ ratios

The presence of the remarkable "M-type" REE tetrad effects in these apatites indicate they are magmatic in origin. As the $^{87}\text{Sr}/^{86}\text{Sr}$ of apatites show no correlations with Eu/Eu^* and $1/\text{Sr}$ (Figures omitted), it implies that the variations of Sr isotope are independent of the magmatic evolution, and no other Sr sources were mixed during the evolution of magmatic system. So, this work takes into account that Sr isotopes of region C apatites result from isotopic exchange with muscovite, or K-feldspar through the pore fluids, and those of region B apatites are related to processes of dissolution or recrystallization of apatites in the Rb-rich fluid, whereas the $^{87}\text{Sr}/^{86}\text{Sr}$ ratios of region A apatites maintain a relative constant and may recorder the initial Sr isotope of magmatic system.

Conclusions: The mechanism controlling unusual high $^{87}\text{Sr}/^{86}\text{Sr}$ ratios in apatites are related to the isotope exchange, and dissolution or recrystallization of apatites in the exsolved magmatic fluid.

Cooling rates and temperature in eruption columns inferred from the hydrous species geospeedometer

YOUXUE ZHANG AND ZHENGJIU XU

Department of Geological Sciences, The University of
Michigan, Ann Arbor, MI 48109-1063, USA

As a volcanic eruption column ascends into the sky, what is the temperature distribution inside the column? We apply a geospeedometer previously developed in this lab (Zhang et al., 1995, 1997, 2000) to investigate cooling rates of pyroclasts in ash beds of the most recent (~1340 AD) eruptions of the Mono Craters (Sieh and Bursik, 1986). Then we use the cooling rates to estimate the temperature in the part of the eruption where and when the pyroclast cooled through its apparent equilibrium temperature (T_{ae}) (that is, when the hydrous species concentrations were frozen in).

Samples of pyroclasts were collected from the Mono Craters ash beds. Unbroken pyroclasts are selected and the size of each estimated. Each sample is then cut and doubly polished. The doubly polished section is analyzed by Fourier transform near-infrared spectroscopy. From each spectrum, the cooling rate at T_{ae} is determined (Zhang et al., 2000).

After obtaining cooling rates as a function of pyroclast size, the results are compared with cooling of obsidian glass in "static" air, allowing us to infer whether the pyroclast cooled through T_{ae} in the eruption column, in flight through air, or in a volcanic bed after deposition. If the pyroclasts cooled through T_{ae} in volcanic beds after deposition, the cooling rates would be independent of clast size but dependent on the position in the beds. If they cooled through T_{ae} in flight through ambient air, the cooling rates would be inversely correlated with clast size and greater than that in "static" air because airflow increases cooling rate. If they cooled through T_{ae} in the eruption column with hot gas surrounding them, the cooling rate would be inversely correlated with clast size but can be less than those in "static" air because the temperature in the eruption column can be high.

Cooling rates of pyroclasts are inversely correlated with sample size and slower than but following a subparallel trend as those in air. Hence we infer that the pyroclasts cooled through T_{ae} in the eruption column. (After cooling through T_{ae} , the pyroclasts cooled further in the column and ash bed to room temperature.) From the cooling rates, we can further infer eruption column temperature in the part of the eruption column where and when the pyroclast cooled through its T_{ae} . They are 230 to 560°C for the most recent eruptions of Mono Craters. The ability to estimate cooling rates and temperature in part of the eruption columns from eruptive products will provide much needed constraints for dynamic models to understand the eruption columns.

The Adakite-like Dacites and Potassic Volcanic Rocks in Chinese Western Tianshan

ZHAO ZHENHUA ; XIONG XIAOLIN ; BAI ZHENGHUA

Guangzhou Institute of Geochemistry, Chinese Academy of Sciences, Guangzhou, P.R. China (zhzhao@gig.ac.cn)

The adakite-like dacites and potassic volcanic rocks (shoshonitic series and high K calc-alkaline rocks) are typical igneous rocks and closely associated in temporal and spatial in Chinese Western Tianshan. They are mainly generated in late Paleozoic Era and the isotopic ages are 330-250 Ma using by ^{40}Ar - ^{39}Ar and K-Ar methods. The adakite-like dacites and subvolcanic rocks (248.7 Ma ~ 260.8 Ma) are somewhat younger.

In the diagram of K_2O versus SiO_2 , the adakite-like dacites and potassic volcanic rocks are plotted in the high K calc-alkaline and shoshonitic area, respectively. For the adakite-like dacites the Al_2O_3 contents are rather high (14.95-16.32) and Na_2O contents are mainly in the range of 5-7%. For the potassic volcanic rocks, the K_2O contents are high with range of 2.0-5.0%. These rocks are generally enriched in highly incompatible trace elements, such as LILE and LREE. The adakite-like rocks are strongly enriched in Sr with the highest concentration >1600 ppm, and strongly depleted in Y with the contents < 10ppm. The Sr/Y ratios are >50 (51-327) and fall right in adakite field and are apparently different from that of volcanic arc andesite and dacite. The REE distribution patterns are characterized by positive Eu anomalies ($\text{Eu}^*/\text{Eu}=1.15$ -1.27), strong HREE depletion and high (La/Yb)_N ratios (17-34). These features show that the adakite-like dacites in Chinese Western Tianshan are similar to those defined by Defant and Drummond (1990,1993).

The variation of ($^{143}\text{Nd}/^{144}\text{Nd}$)_i and ($^{87}\text{Sr}/^{86}\text{Sr}$)_i of the adakite-like dacites are small: 0.51236-0.51248; and 0.7052-0.7054, respectively. The eNd(T) values are positive (1.98-4.23) and eSr(T) values are low positive (15.7-17.3). For the potassic volcanic rocks the Nd and Sr isotopic compositions are very similar to those of adakite-like dacites, the ($^{143}\text{Nd}/^{144}\text{Nd}$)_i and ($^{87}\text{Sr}/^{86}\text{Sr}$)_i values fall in the range of 0.51232-0.51261 and 0.7041-0.7054, with eNd (T) and eSr (T) values of +1.28-+3.38 and $\bar{n}0.45$ -+18 respectively. On the diagram of ($^{87}\text{Sr}/^{86}\text{Sr}$)_i -e Nd(T) the adakite-like and potassic rocks are all fall into the first quadrant. This is similar to the island arc type of volcanic rocks in the Lesser Antilles and Sunda Arc. This suggests that the adakite-like and potassic volcanic rocks in Chinese Western Tianshan area may have been derived from similar source -mantle-derived with slight enrichment.

The trace element associations of these igneous rocks all show that they are mainly occurred in the continental arc and post collision arc tectonic settings and it could provide evidences for the regional Paleozoic geodynamic evolution.

A large scale of meteoric-hydrothermal alteration at Neoproterozoic in the Yangtze craton of China

YONG-FEI ZHENG, BING GONG, LONG LI AND WEI-MIN FENG

School of Earth and Space Sciences, University of Science and Technology of China, Hefei 230026, China (yfzheng@ustc.edu.cn)

Since anomalous low $\delta^{18}\text{O}$ values of -10 to -8‰ were discovered for ultrahigh pressure (UHP) eclogite at Qinglongshan in the Sulu terrane, a cold paleoclimate was inferred to occur at Neoproterozoic. This provides an important constraint on the ongoing debate about the hypothesis of "snowball earth". Because protoliths of granitic orthogneiss and most eclogites in the Dabie-Sulu orogen are of igneous origin, an extended study of the UHP rocks by means of zircon oxygen isotope analysis and U-Pb dating is carried out to identify the timing and areal distribution of the meteoric-hydrothermal alteration.

CO_2 laser fluorination analysis on 112 zircon samples from the UHP rocks shows $\delta^{18}\text{O}$ values of -10.3 to +5.6‰ in the Sulu terrane and -4.6 to +8.9‰ in the Dabie terrane. The analysed samples cover most regions of the Dabie-Sulu orogen, with an outcrop area of over 15,000 km². Almost a half of the zircon samples have the lower $\delta^{18}\text{O}$ values than the normal mantle zircon 5.3 ± 0.3 ‰, indicating the involvement of surface fluids in the formation of the UHP rocks. In particular, the low- $\delta^{18}\text{O}$ magmas are expected for the protoliths of the UHP rocks.

Over 50 zircon U-Pb datings from either upper intercept of Wetherill-type discordia or ionprobe single $^{206}\text{Pb}/^{238}\text{U}$ point shows an age range of 600 to 880 Ma with a mode of 730 to 790 Ma for protoliths of most eclogites and orthogneisses in the Dabie-Sulu orogen. These ages may correspond to rift-magmatic events in the northern margin of the Yangtze craton. They are also correlated with the sedimentation timing of the Nantuo tillites on the Yangtze platform. The ^{18}O -depleted fluid may be associated with the Neoproterozoic glaciations in a fashion of either cold paleoclimate or melting of snow or glacier ice.

Because meteoric water is the only source of ^{18}O -depleted fluids on the Earth, it is commonly assumed that low $\delta^{18}\text{O}$ values for igneous and metamorphic rocks are produced by meteoric-hydrothermal alteration at high temperatures. Alternatively, melting of glacier ice is proposed to produce the ^{18}O -depleted fluids, and the Neoproterozoic rift-magmatism in the northern margin of the Yangtze craton is considered as the heat source that melts the glacier ice to trigger the water-rock interaction. Therefore, the widespread occurrence of the negative $\delta^{18}\text{O}$ values for the zircons of the Neoproterozoic ages are a manifestation of the snowball Earth at that time.

Disequilibrium Sm-Nd and O isotope systems in garnet peridotite during UHP metamorphism

YONG-FEI ZHENG¹, JIAN-JUN YANG², BING GONG¹
AND BOR-MING JAHN³

- ¹. School of Earth and Space Sciences, University of Science and Technology of China, Hefei 230026, China (yfzheng@ustc.edu.cn)
- ². Institute of Geology and Geophysics, Chinese Academy of Sciences, Beijing 100029, China
- ³. Geosciences-Rennes, Université de Rennes 1, Campus de Beaulieu, 35042 Rennes Cedex, France

In the isotopic geochronology of metamorphic rocks, an critical question is whether radiometric systems of mineral isochron have achieved thermodynamic equilibrium during a given metamorphic event and preserved the equilibrium afterwards. A garnet peridotite at Zhimafang in the Sulu terrane of eastern China shows decoupled Sm-Nd, Rb-Sr and U-Pb systems when making radiometric dating. Two samples of mineral Sm-Nd isochron yield ages of 376 ± 14 Ma and 378 ± 24 Ma, respectively. Mineral Rb-Sr isochron dating gives consistent ages of 201 ± 4 Ma and 205 ± 4 Ma for the same two samples. SHRIMP zircon U-Pb dating gives discordant ages of 216 to 233 Ma, but an isochron age of 224 ± 8 Ma. Sm-Nd isotope disequilibrium is suggested among the minerals if the Triassic UHP metamorphic event is assumed for the garnet peridotite. This is confirmed by petrological textures and the state of oxygen isotope equilibrium or disequilibrium among the constituent minerals in the garnet peridotite.

Oxygen isotope disequilibria are observed among most minerals. In particular, garnet is not in oxygen isotope equilibrium with any other of the analysed minerals. The degree of oxygen isotope disequilibria between the other minerals varies from pair to pair. Oxygen isotope equilibrium is only observed between orthopyroxene and olivine for both samples and between phlogopite and clinopyroxene for one sample. The $\delta^{18}\text{O}$ values of both single minerals and whole-rock for the two isochron samples fall within the $\delta^{18}\text{O}$ range of $5.7 \pm 0.5\text{‰}$ for the normal mantle, indicating that the garnet peridotite was not significantly affected either by meteoric-hydrothermal alteration before plate subduction like the UHP eclogites in this region.

This combined study of U-Pb, Rb-Sr, Sm-Nd and O isotope systems demonstrates that the duration of the UHP metamorphism and subsequent HP eclogite-facies recrystallization was not long enough for the reequilibration of the Sm-Nd and O isotope systems in the garnet peridotite, but just long enough for the reequilibration of the Rb-Sr isotope systems. The timescale of the Rb-Sr reequilibration is thus shorter than that of the Sm-Nd and O isotope reequilibration at mantle and deep-crustal depths. Therefore, the rates of Sr isotope reequilibration between the mafic minerals are constrained to be faster than those of Sm-Nd and O isotope reequilibration between the same minerals at the mantle and deep-crustal conditions.

Oxygen isotope mapping of UHP metamorphic rocks in the Dabie-Sulu orogen of China

YONG-FEI ZHENG, LONG LI, ZI-FU ZHAO AND
BING GONG

School of Earth and Space Sciences, University of Science and Technology of China, Hefei 230026, China
(yfzheng@ustc.edu.cn)

Metamorphic devolatilization is very common during subduction of oceanic crusts because of the presence of fluid-rich marine sediments. However, it is a question whether subduction of a continental crust also produces a great deal of volatiles during prograde metamorphism. Occurrence of diamond and coesite in supracrustal rocks in the Dabie-Sulu orogen provides an important target to study fluid mobility during UHP metamorphism of the Yangtze continental plate.

Oxygen isotope mapping was accomplished for various types of HP and UHP rocks, including eclogite, granulite, paragneiss and granitic orthogneiss, over an outcrop area of about 15,000 km² in the Dabie-Sulu orogen. Despite a large variation in $\delta^{18}\text{O}$ value from -10 to $+10\text{‰}$ for the UHP rocks, ^{18}O depletion relative to the normal mantle is discovered in most regions of this orogen. Most of the samples have preserved oxygen isotope equilibrium fractionations between quartz and the other minerals, suggesting that these rocks acquired the low $\delta^{18}\text{O}$ signature before plate subduction.

Heterogeneous $\delta^{18}\text{O}$ distribution in the eclogites and gneisses is observed not only in the regional scale (-8 to $+10\text{‰}$ in the Shuanghe area of eastern Dabie, and -10 to $+5\text{‰}$ in the Donghai area of western Sulu) but also in outcrop scales (for instance, at Bixiling in eastern Dabie and at Qinglongshan in western Sulu). While a small variation in $\delta^{18}\text{O}$ from -11.1 to -10.1‰ is observed for garnet within 5 to 6 m distances from kyanite-bearing eclogite at the western outcrop of Qinglongshan, there are large $\delta^{18}\text{O}$ variations from -5.5 to -1.6‰ for garnet within 2 to 3 m distances from the epidote-bearing eclogite at the eastern outcrop of Qinglongshan and from -1.8 to $+3.8\text{‰}$ for garnet within 200 m outcrop from the Bixiling eclogite. In some localities, oxygen isotope homogenization between different rock types was limited to distances of 10 cm, and little or no effective isotopic transport took place over distances greater than 1 m.

The present study demonstrates very small mobility of fluids during UHP metamorphism of the continental crust. The UHP metamorphism is characterized by channelized fluid flux; slab fluids originate from the metamorphosed supracrustal rocks whose protoliths were hydrothermally altered by the fluid of meteoric water origin; oxygen isotope composition of the fluid is heterogeneous within the subducted slab; the fluid flux is low during the prograde and peak UHP metamorphism. Therefore, the extremely ^{18}O -depleted signature of pre-subduction fluid-rock interactions is not only well preserved in the UHP rocks but also carried into the Earth's interior by broken off slab.

Longevity and multistage evolution of subcontinental lithospheric mantle beneath eastern China: evidence from Re-Os isotope geochemistry of mantle peridotite xenoliths from Jiangsu and Anhui Provinces, China

X.C. ZHI¹ L. REISBERG² C. WAGNER³ Z.C. PENG¹ AND X. S. XU⁴

¹. Department of Earth and Space Sciences, University of Science and Technology of China, Hefei, 230026 China (xczhi@ustc.edu.cn), (pzc@ustc.edu.cn)

². CRPG/CNRS, BP20, 54501 Vandoeuvre-lès-Nancy Cedex, France (reisberg@crpg.cnrs-nancy.fr)

³. Laboratoire PMMP, Université Paris 6, 4Place Jussieu, 75252 Paris Cedex 05, France (cw@ccr.jussieu.fr)

⁴. Department of Earth Sciences, Nanjing University, Nanjing, 210093, China (xxu@public1.ptt.js.cn)

The Cenozoic alkaline basalts of eastern China contain many mantle peridotite xenoliths. One of the most important locations is the area along the boundary of Anhui and Jiangsu provinces, part of the continental subduction-collision zone between the North China and Yangtze tectonic plates. We present Re-Os results from more than 40 samples collected in Nushan in Anhui province and Pengshishan, Nanliangshan and Fangshan in Jiangsu Province. The samples are mostly anhydrous spinel lherzolites, but also include spinel harzburgites, spinel-garnet lherzolites and modally metasomatized spinel lherzolites including amphibole-, biotite- and apatite-bearing varieties. Except for the Nushan samples, which are more deformed, most samples have protogranular to slightly porphyroclastic textures. Major element compositions vary systematically from fertile to depleted in basaltic components such as Al_2O_3 , CaO, TiO_2 and Na_2O . REE patterns vary from LREE enriched to highly LREE depleted, with the modally metasomatized lherzolites displaying highly fractionated REE patterns.

Re and Os abundances vary from 0.018 to 0.375 ppb and from 0.921 to 3.35 ppb respectively. $^{187}Os/^{188}Os$ ratios range from 0.115 to 0.134, in concert with indices of melt extraction such as Al_2O_3 , Yb and Lu contents. The Os data indicate a Middle Proterozoic melt depletion age for the lithospheric mantle in the area. This suggests that the shallow spinel lherzolite mantle represented by most of the samples is the remnant of old Proterozoic mantle remaining after delamination. Interestingly, spinel-garnet lherzolites with high equilibration temperatures, found only in Nushan, have both fertile major element compositions and Os isotopic ratios similar to that of the primitive upper mantle. This may indicate that material newly accreted from the asthenosphere has been added beneath the shallow spinel lherzolite, in agreement with tectonic models of the region.

The law of gold activities in alkaline basaltic magma: Evidence from high temperature and ultrahigh pressure experiments

HUANG ZHILONG ZHU CHENGMING LU LONGFANG

Institute of Geochemistry, CAS, Guiyang 550002

It is approved by many large and super-large gold deposits that lamprophyres are temporally and spatially related to gold mineralization [1]. There is controversy whether lamprophyric magma provide gold or not in the processes of gold mineralization. The alkaline basaltic magma can be considered as the parent magma of lamprophyres [2]. We carried out the melting experiments of alkaline basalts + gold at high temperature and ultrahigh pressure, and discussed the law of gold activities in alkaline basaltic magma.

The experimental starting materials are alkaline basaltic powder with grain size less than 0.09 mm which were immersed with gold-bearing solutions for 1 h and dried. The content of gold in starting materials is 51 ppb. A DS-29A cubic-type 3600t ultrahigh-pressure apparatus was employed for the experiment. The experimental procedure is the same as Huang et al. .

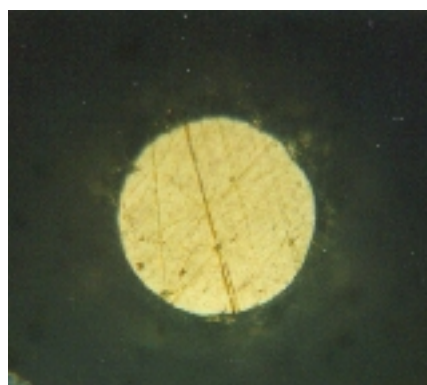


Fig.1 Experimental results of alkaline basalts + gold. 63°;10, 1.5GPa, 1450°CÊ.

The melting experiments of alkaline basalts + gold at 1.5GPa-3.0GPa and 1400°CÊ-1500°CÊ are carried out and the experimental results show good reproducibility under the same conditions. The experimental results showed that the gold in starting materials assembled to be gold balls and precipitated to the bottom of the experimental products. The boundary lines between the gold ball and the alkaline basaltic glass were distinct (Fig. 1). The alkaline basaltic magma can be considered as the parent magma of lamprophyres [2]. Our Experimental results show that the gold in the alkaline basaltic magma in chamber would assemble to be gold balls and precipitate to the bottom of chamber by gravity.

So, the gold contents in ascending lamprophyric magma which is product of evolution of alkaline basaltic magma is little. That is to say, the possibility of lamprophyric magma to provide gold in the processes of gold mineralization is little.

[1] Rock N M S, et al. *Nature*, 1988, 332: 253-255. [2] Huang Z L, et al. *Geochem J*, 2002, 36: 96-103. [3] Huang Z L, et al. *Chinese Sci Bull*, 1999, 44: 2073-2076

Evaluation of Ar-Ar ages of Individual Mica Grains for Provenance Studies of Loess, Long Island, NY

JIAN ZHONG¹, SIDNEY R. HEMMING², AND GILBERT N. HANSON³

¹Department of Geosciences, SUNY, Stony Brook, NY 11794-2100 (jian@pbisotopes.ess.sunysb.edu)

Lamont Doherty Earth Observatory, Palisades, NY 10964 (sidney@lamont.ligo.columbia.edu)

³Department of Geosciences, SUNY, Stony Brook, NY 11794-2100 (gilbert.hanson@sunysb.edu)

Loess was studied on the SUNY Stony Brook Campus and from Caumsett State Park 40 Km to the west. The loess was deposited after the last glacier retreated from Long Island some 20,000 years ago. The loess overlies till and there are no overlying sediments. The loess on the SUNY Stony Brook Campus has three modes: fine sand (250 microns), silt (20 microns), and clay (<2 microns). The sand in the loess is probably wind blown sand.

The occurrence of wind blown sand suggests that the loess was transported by strong katabatic winds flowing off the glacier to the north. Long Island is a good place to evaluate mica ages for provenance studies of loess derived by a glacier from local bedrock because the Ar-Ar and K-Ar mica ages in the bedrock north of Long Island change essentially continuously from New Jersey and New York in the west to New England in the east, from 900 to 200 Ma respectively.

Lewis and Stone, 1991, suggest that a glacial lake occupied the Long Island Sound basin to the north of Long Island as the last glacier retreated. Streams carried glacial sediments to the lake from Connecticut and areas to the north. As the level of the glacial lake lowered, the glacial sediments deposited in the lake were exposed and may be a dominant local source for the loess.

Muscovite ages for the loess from Caumsett State Park range from 275 to 375 Ma. Muscovite ages for loess on the Stony Brook campus are somewhat younger dominantly 225 to 300 Ma. The younger ages are consistent with a more easterly source. One grain of muscovite has an age of 1002 Ma, suggesting that it may have a source further to the west.

Ages for biotite from the loess range from 44 to 1804 Ma with the majority between 250 to 400 Ma. Some of the biotite ages range from 500 to 850 Ma consistent with derivation from Grenville sources to the west. Biotite with ages greater than 1100 Ma most likely has a mid-continental source to the west. Some of the biotite grains with ages younger than 200 Ma may have been affected by weathering.

These results suggest that the micas were derived mostly from the north or west, consistent with transport by prevailing westerly winds or southerly katabatic winds. The use of single grain mica Ar-Ar dating is a promising method for provenance study of loess.

Reference

Lewis RS, and Stone JR, (1991) Jour. Coastal Research, Spec. Issue No. 11, 1-23.

Oxygen isotope fractionation between aragonite and water at low temperatures

GEN-TAO ZHOU AND YONG-FEI ZHENG

School of Earth and Space Sciences, University of Science and Technology of China, Hefei 230026, China (yfzheng@ustc.edu.cn)

Calcium carbonate is one of the most important minerals in reconstructing ocean paleotemperature by means of oxygen isotope analysis. However, significant discrepancies in oxygen isotope fractionation factors between two CaCO₃ polymorphs, calcite and aragonite, have been observed for the data from theoretical calculations, experimental measurements, and natural observations. The purpose of this study is to investigate the influence of carbonate precipitation rate on oxygen isotope fractionation by chemical synthesis experiments, and to determine the equilibrium fractionation factors between aragonite and water during inorganic precipitation of CaCO₃.

The experiments were carried out by means of the slow precipitation method, in which the Ca(HCO₃)₂ solutions were prepared either by dissolving solid CaCO₃ or NaHCO₃ in aqueous solutions. The phase compositions and morphologies of synthetic minerals were detected by XRD and SEM techniques. The effects of aragonite precipitation rate and excess dissolved CO₂ gas in the initial Ca(HCO₃)₂ solution on oxygen isotope fractionation between aragonite and water were investigated. For the CaCO₃ minerals slowly precipitated by the CaCO₃ or NaHCO₃ dissolution method at 0 to 50°C, the rate of aragonite precipitation increased with temperature. Correspondingly, oxygen isotope fractionations between aragonite and water deviated progressively farther from equilibrium. In addition, an excess of dissolved CO₂ gas in the initial Ca(HCO₃)₂ solution results in an increase in apparent oxygen isotope fractionations. As a result, the experimentally determined oxygen isotope fractionations at 50°C indicate disequilibrium, whereas the relatively lower fractionations obtained at 0 and 25°C from the solution with less dissolved CO₂ gas and low precipitation rates indicate a closer approach to equilibrium.

Combining those lower values at 0 and 25°C in this study with data derived from the two-step overgrowth technique at 50 and 70°C (Zhou and Zheng, 2002), a fractionation equation for the aragonite-water system at 0 to 70°C is obtained as follows:

$$10^3 \ln \alpha = 20.44 \times 10^3 / T - 41.48.$$

Discussion concerning the kinetic mechanism of oxygen isotope disequilibrium argues for this equation to be a close proxy for thermodynamic equilibrium fractionation in the low-temperature mineral. Therefore, the discrepancies in CaCO₃-H₂O fractionation factors between different published synthesis experiments may reflect steady-state equilibrium fractionations obtained during aragonite precipitation and subsequent polymorphic transition to calcite at different run conditions.

References

Zhou G.-T. and Zheng Y.-F. (2002) *Geochim. Cosmochim. Acta*, 66, 63-71.

Local response to global Mesozoic overturn: Inferred from SHRIMP zircon dating of lower crust xenoliths, North China Craton

XINHUA ZHOU¹, S.A. WILDE², MIN SUN³ AND A.A.NEMCHIN²

1. Institute of Geol. and Geophys., Chin. Acad. Sci., Beijing 100029, China (zhouxh@public3.bta.net.cn)
2. Curtin University of Technology, GPO Box U1987, Perth, West Australia, 6845 (wildes@lithos.curtin.edu.au)
3. Dept. Earth Sciences., Hong Kong University, Pokfulam Road, Hong Kong, China (minsun@hkucc.hku.hk)

The large scale subcontinental lithosphere thinning beneath North China Craton in Mesozoic-Cenozoic is well recognized as a major geodynamic process in eastern China, especially in the eastern part of North China Craton, but there has always been controversy as to when and what the timing, mechanism and consequence related to this event is. Based on a systematic study on granulite and pyroxenite xenoliths entrained in Neogene basalts, North China Craton, with emphasize on SHRIMP U/Pb dating of zircons, we hereby present direct geochronological evidence for timing of basaltic underplating, fractional melting and magma cumulate. Although the entire data sets display a complicated and multiple-peak spectrum, which prominently defines a broad peak of activity between 80 and 120 Ma and, the peak around 160 to 180 Ma in the duration of Mesozoic. They would be responsible for the surface expression of Late Mesozoic intensive and voluminous granitoids, volcanic rocks, diorites, dikes and widespread gold mineralization in that region. It reflects the multiple episodic thermal perturbation beneath North China Craton, resulting in major transformation of architecture of subcontinental lithosphere. It is inferred that the global cretaceous catastrophic geodynamic process in deep mantle, most likely, would coincide with, and then, should be responsible for these events.

Noble gas tracing of coalbed methane generation and biomodification

Z. ZHOU¹, C. J. BALLENTINE², R. KIPFER³, M. SCHOELL⁴ AND S. THIBODEAUX⁵

- ¹ IGMR, ETH Zurich, Switzerland (zhou@erdw.ethz.ch)
- ² The University of Manchester, Manchester, United Kingdom (cballentine@fs1.ge.man.ac.uk)
- ³ EAWAG, Zurich, Switzerland (rolf.kipfer@eawag.ch)
- ⁴ Chevron Research and Technology Company, San Ramon, USA (mrtn@chevron.com)
- ⁵ Burlington Resources, Farmington, USA (sthibodeaux@br-inc.com)

Fractured coalbeds can provide a commercial methane gas resource and because of their high sorptive gas capacity are a potential target for CO₂ sequestration projects. The San Juan Basin is located on the eastern margin of the Colorado Plateau, USA. Biodegradation of the Late Cretaceous coal seams produces one of the world's largest non-conventional methane natural gas resources. The highest regions of gas production correlate with changes in groundwater chemistry indicative of recent groundwater involvement in the coal biodegradation. Furthermore, in the high gas production regions spatially coherent changes in CO₂/CH₄ ratios correlate with δ¹³C(C₂) and C₂ content. These can be fitted to a simple Rayleigh fractionation model and has been interpreted as biomodification of the natural gas composition.

Noble gases from groundwater are isotopically distinct, and their elemental abundance pattern is only changed by physical processes. Noble gases can therefore play a dual role in both quantifying the role of the groundwater system in the biodegradation process as well as resolving compositional and isotopic fractionation caused by sorption/desorption from the coal surfaces.

26 samples have been collected for compositional, stable isotope and noble gas determination. 8 of these are from a region showing no coal bed biodegradation. These provide a control and show a coherent increase in ⁴⁰Ar/³⁶Ar, ³He/⁴He and ²¹Ne/²²Ne ratios, from 384 to 625, 0.0836Ra to 0.168Ra and 0.0213 to 0.0343 respectively, with distance from the basin margin. Groundwater-derived noble gas concentrations (²⁰Ne, ³⁶Ar, ⁸⁴Kr and ¹³⁶Xe) all decrease with increasing distance from recharge. Preliminary results from the high production/biodegraded regions show concentrations of atmosphere-derived noble gases up to three orders of magnitude lower than the control. These gases are highly fractionated with ²⁰Ne < ³⁶Ar < ⁸⁴Kr < ¹³⁶Xe relative to groundwater values. These results are interpreted as a combined effect of dilution and fractionation caused by desorption of gases from the coal during production.

References

- Scott A.R., et al., (1994), *AAPG Bull.* **8**, 1186-1209.
Ballentine C.J., et al., (1991), *EPSL* **105**, 229-246.

Calculation of the strain, stress and elastic energy for low-high quartz transition up to 1.1GPa

W-G ZHOU¹ H-S XIE¹ Z-D ZHAO²

¹Laboratory of Geodynamic under High Temperature and Pressure, Institute Geochemistry, Chinese Academy of Sciences, Guiyang, China (zhouwg@sohu.com)

²Department of Geology, China University of Geosciences (Beijing), Beijing, China (zhidanz@cug.edu.cn)

Considering all the rock-forming minerals in the crust, quartz is probably the most abundant one. The physical and chemical properties of quartz have been extensively investigated. This paper is particularly concerned with the strain, stress and elastic energy in low-high quartz transition at the pressure range of crust.

Procedure of Calculation

As the low-quartz is transformed into high-quartz, the components (e_i) of the strain tensor is: $e_1 = e_2 = a / a_0 - 1$, $e_3 = c / c_0 - 1$, $e_4 = e_5 = e_6 = 0$, where a_0 and c_0 are the cell parameters of low-quartz, and a and c are the cell parameters of high-quartz.

The relationship between an applied stress, σ_i , and the resultant strain, e_k , and the temperature, T , is given by the generalized Hook's law: $\sigma_i = C_{ij}e_j - C_{ij}\alpha_j T$, where C_{ij} are the elastic constants, α_j are thermal expansivities. The elastic energy, G , stored in the crystal is:

$$G = 1/2 \sum_{i,k} C_{i,k} e_i e_k$$

The variations of the lattice parameters of low- and high-quartz at high pressure and high temperature can be evaluated with the compressional and thermoelastic properties of low- and high-quartz. Combined the boundary of low-high quartz transition with the results of evaluation, the lattice parameters of low- and high-quartz at their transition pressure and temperature are determined firstly. Then, the strains, stresses and elastic energies for low-high quartz transition were calculated according to Hooke's law with the aid of the elastic constants of high quartz.

Results and Discussion

The results indicate that at the pressure of 0-1.1 GPa, the strains for low-high quartz transition are varied in the range of -0.006-0.005, the stresses in the range of -0.46-0.14 GPa, and the elastic energies in the range of 965-2760 kJ / m³. At about 0.5 GPa, the strains, stresses and elastic energies achieved their minimum values. Based on the calculation, the effect of the low-high quartz transformation on the wall rock is significant in the crust during the acid magma intrusion.

Reference

Carpenter, M. A., Salje E. K. H., and Graeme-Barber A., (1998), *Eur. J. Mineral.* 10, 621-691.

Groundwater Recharge in Late Pleistocene and Holocene at Yucca Mountain, Nevada USA

CHEN ZHU^{1*}, JAMES R. WINTERLE², AND ERICA I. LOVE¹

¹Department of Geology and Planetary Science, University of Pittsburgh, Pittsburgh, PA 15260, USA

²Center for Nuclear Waste Regulatory Analyses, Southwest Research Institute, 6220 Culebra Road, San Antonio, TX 78238, USA

The deep unsaturated zone beneath Yucca Mountain is proposed as the site of a geologic repository for high-level nuclear waste in USA. Reliable estimates of recharge at the local scale are important because infiltrating waters provide a potential means for mobilization of radionuclides. The chloride mass balance (CMB) method has been used for estimating groundwater recharge at Yucca Mountain. CMB is economic and effective, provided that the hydrological conditions for its applications are met and the modeling parameters are known. However, modeling parameters such as precipitation and Cl⁻ deposition rates vary temporally, most notably as a result of the drastic climatic changes from late Pleistocene to Holocene. A common practice in the application of the CMB method is to use present day average precipitation and effective Cl⁻ deposition rates to calculate recharge rates without regard to the age of the groundwater. This study shows that Cl⁻ deposition rates, estimated from ³⁶Cl data, were lower in late Pleistocene than Holocene at Yucca Mountain, Nevada, but higher in late Pleistocene than Holocene at Black Mesa, Arizona, another arid environment where hydrological data are abundant.

Temporal variability of atmospheric Cl⁻ input, as well as annual precipitation, was considered in this study to estimate recharge rates using the CMB method. The resulting average recharge estimates for Black Mesa are 9 mm/yr for Holocene and 35 mm/yr for late Pleistocene. Local recharge rates at Yucca Mountain were estimated from the ³⁶Cl/Cl ratios and Cl⁻ concentrations in perched waters. The estimated recharge for Yucca Mountain is 5 mm/yr for Holocene and 15 mm/yr for late Pleistocene. Although there is uncertainty in these estimates, greater confidence can be placed in the relative rates of recharge estimated for the late Pleistocene and the Holocene. These estimates agree well with spatially and time-averaged net infiltration estimates for present-day and glacial-transition climates (4.6 mm/yr and 15.6 mm/yr, respectively) obtained from a watershed-scale infiltration model of Yucca Mountain. [This work, performed in part under U.S. Nuclear Regulatory Commission (NRC) contract NRC-02-97-009, does not necessarily reflect views or position of the NRC.]

Occurrence of native selenium in Yutangba of China

J.M. ZHU, X.B. LIANG, B.S. ZHENG AND S.H. LI

State Key Lab. of Environmental Geochemistry, Institute of Geochemistry, Chinese Academy of Sciences, Guiyang 550002, P.R.China (jmzhu@mailcity.com)

Yutangba, located in northern part of Shuanghe Town of Enshi City in the SW of Hubei Province, China, is the unique location in the world where local villagers widely suffered from selenosis in 1963^[1]. In Yutangba, Se-rich rocks ("stone coal" named by local residents) are mainly carbonaceous siliceous rock and siliceous carbonaceous shale of the Lower Permian Maokou Formation. The rock samples have a maximum Se content of 84123mg/kg^[1], but little is known about the modes of occurrence of Se in Se-rich rocks.

The result of our studies by using SEM-EDX, electronic microprobe and X-ray diffraction shows that native Se, which varies morphologically due to different mechanisms, was found within the abandoned stone coal spoils and Se-rich carbonaceous siliceous rock. Genetically, native Se is mainly divided into three types, which are derived from natural burning of stone-coal, weathering and tectonic activity. But based on its occurring environments, native Se can be divided into five kinds. The first is produced near the subsurface of abandoned stone coal spoils with well developed crystal morphology and the grain size up to 28mm. The second is closely associated with quartz and carbonaceous matter with good crystal morphology but very small grain size as micro-needles. The third as micro-acicular crystals, found in the highly carbonaceous mudstone. The fourth is formed from weathering of Se-rich rocks, Se-bearing minerals (such as pyrite) and surface redox of the larger Se crystals. The fifth is elemental Se (Se⁰) or selenides with microorganism morphology, only found in the carbonaceous siliceous rock.

Native Se is first found in such a small landscape in China that Se crystals produced are so large in scale, and the occurrence of native Se in Yutangba would be helpful to further study mineralogy, environmental geochemistry of Se in stone coal and its effect on the local environment.

References

Yang G.Q., Wang S.Z., Zhou R.H. and Sun S.Z., (1983), *Am. J. Clin. Nutr.* 37, 872-881.

Spatial and temporal variations of transition metal isotopes in Oceans

X.K. ZHU, Y. GUO AND R.K. O'NIONS

Department of Earth Sciences, Oxford University, Parks Road, Oxford, OX1 3PR, UK (Xiangz@earth.ox.ac.uk)

The transition metals Cu, Zn and Fe are present as trace elements in seawater, but are biologically utilised. It is anticipated that the isotope compositions of these elements in seawater will be a function of several factors including their source input, ocean circulation and biological processing. Isotopic variations of these elements may in turn be used to reconstruct details of these processes, particularly in relations to climate changes.

Samples selected for this study are Fe-Mn crusts from world-wide oceans. Hydrogenous Fe-Mn crusts has proved to provide excellent records of isotope compositions of dissolved metals in deep seawater (O'Nions et al., 1997; Zhu et al., 2000a). The investigation on transition metal isotopes was performed on surface samples and as depth-profiles (time series). Fe, Cu and Zn isotopes were measured using a Nu Instruments MC-ICPMS after chemical purification (Zhu et al, 2000b, 2002). Results are expressed in ϵ units which are deviations in parts per 10⁴ from the isotope reference materials.

The Fe, Cu and Zn isotopes of deep seawater deduced from the Fe-Mn crusts show both spatial and temporal variations. For Fe isotopes, an overall variation of ca. 20 $\epsilon^{57}\text{Fe}$ units has been observed from the surface samples. Whereas relatively large intra-ocean variation has been observed (e.g. Atlantic: $-13.9 \leq \epsilon^{57}\text{Fe}_{\text{IRMM14}} \leq 6.6$), the average Fe isotopes composition for each Ocean are remarkably similar. But they are significantly enriched in light isotopes relative to both the continental and oceanic crusts. Comparing with Fe isotopes, variations for Cu and Zn isotopes are much smaller. Like Fe isotopes, no inter-Ocean differences in Cu and Zn isotopes have been observed.

Besides the surfaces samples, a high resolution time-series of Fe, Cu and Zn isotopes has been obtained from a North Atlantic Fe-Mn crust, which demonstrates that the Fe, Cu and Zn isotope compositions in North Atlantic Deep Water have changed substantially over the last 6 Ma. Moreover, it has been observed that the Fe-isotope variations in the crust are closely correlated to those of Pb-isotopes, which indicates that the observed Fe-isotope variations predominantly reflect those of Fe input from terrigenous sources. But the profiles of Cu- and Zn-isotopes contrast greatly to those of Fe- and Pb-isotopes, whereas Cu- and Zn-isotopes themselves show remarkably similarity. This suggests that the recorded Cu and Zn isotope variations result predominantly from processing within Oceans themselves.

References

O'Nions, R.K. et al, (1997), *Earth Planet. Sci. Lett.* 155, 15-28.
 Zhu, X.K. et al, *Science* (2000a), 287, 2000-2002.
 Zhu, X.K. et al., (2000b), *Chem. Geol.* 163, 139-149.
 Zhu, X.K. et al., (2002), *Earth Planet. Sci. Lett.* 200, 47-62.

The $\delta^{30}\text{Si}$ values of soil weathering profiles: Indicators of Si pathways at the lithosphere/hydro(bio)sphere interface

K. ZIEGLER¹, O.A. CHADWICK¹, E.F. KELLY² AND M.A. BRZEZINSKI³

¹ Dept. of Geography, University of California, Santa Barbara, CA 93106, USA (kziegler@geog.ucsb.edu, oac@geog.ucsb.edu)

² Dept. of Soil and Crop Sciences, Colorado State University, Ft. Collins, CO 80523, USA (pedoiso@lamar.colostate.edu)

³ Dept. of Ecology, Evolution and Marine Biology, University of California, Santa Barbara, CA 93106, USA (brzezins@lifesci.ucsb.edu)

We utilize natural variations in the abundance of Si isotopes to trace the fate of Si derived from weathering of rock in terrestrial ecosystems. Previous experimental work has indicated that phytolith (plant opal) and clay mineral formation create relatively large Si-isotopic differences between solution and solid (up to -1.5‰). Assuming simple Rayleigh-type fractionation as bedrock is converted to secondary mineral phases and as plants utilize the Si in soil-water, we expect the $\delta^{30}\text{Si}$ variations to increase. Hence, natural variations in silicon isotopes may be a useful tool for assessing the relative contribution of weathering and plant activity in silicon cycling within soils.

A detailed investigation of the Si-budget/transfer between the soil- and the biomass-pool of an arid soil (Kohala/Hawaii, basalt) demonstrates that Si-uptake by plants plays a substantial role in the Si-cycling of this 1-m thick soil. Basaltic groundwater (1500') has a $\delta^{30}\text{Si}$ -value of +0.5‰. Soil-water from the lower B-horizon has a similar value, whereas upper B- and A-horizon soil-waters are more positive by up to 1.2‰. The ^{30}Si -enrichment of solutions relative to groundwater is accompanied by a ^{30}Si -depletion in the precipitating solid phases: secondary halloysite has a $\delta^{30}\text{Si}$ -value of -2.3‰, and phytoliths range from -0.9 to -1.5‰.

Similar clay mineral/soil-water relationships are seen in a several-m-thick saprolite at the humid granitic LTER site of Rio Icacos/Puerto Rico. $\delta^{30}\text{Si}$ -values of secondary kaolinite increase with depth from -2.5 to -1.9‰, whereas soil-water has a value of -0.8‰. Remaining primary quartz has a uniform $\delta^{30}\text{Si}$ signature of -0.2 to -0.3‰.

Our Si isotope values from rock-water-biomass-systems suggest that Si isotope compositions result from the combined effects of dissolution of primary and recycled secondary minerals and inorganically and organically mediated precipitation of new phases. Once these isotopic interconnections are resolved, we will be able to determine duration and intensities of past and recent biogeochemical processes affecting Si-budgets in weathering environments.

Late Pleistocene variations of lake level and glacial activity at Mono Lake, CA, USA

S.R.H. ZIMMERMAN, S. R. HEMMING, N. G. HEMMING, P. B. TOMASCAK

Dept. of Earth & Env. Sciences and Lamont-Doherty Earth Obs., Columbia U., NY, NY 10027; (herrzim@ldeo.columbia.edu) and (sidney@ldeo.columbia.edu)

School of Earth & Env. Sciences, Queens College, Flushing, NY 11367; (hemming@ldeo.columbia.edu)

Dept. of Geology, U. of Maryland, College Park, MD 20742; (tomascak@geol.umd.edu)

Sediments of the Wilson Creek Formation (Marine Isotope Stages 4-3-2) record the details of glacial variation in the Mono Basin, at the eastern foot of the Sierra Nevada in east-central California, USA. Preserved in the deep lake silts of the Wilson Creek Formation, Total Inorganic Carbon (wt. %TIC) and $^{87}\text{Sr}/^{86}\text{Sr}$ of ostracod shells record variations in the lake level related to changes in precipitation/evaporation (P/E). During periods of low P/E, conditions were similar to modern; carbonate precipitated immediately upon mixing of Ca^{2+} -rich waters with CO_3^{2-} -rich lake water, yielding low %TIC (<1%) in deep lake sediments. Sr isotopic ratios were relatively high (0.7093), due to a dominance of Sierran run-off. Conversely, periods of high P/E (high lake level), were characterized by high %TIC (4-6%) and lower $^{87}\text{Sr}/^{86}\text{Sr}$ (0.7089), due to greater influence of Quaternary volcanics in the eastern side of the basin.

Rafting of coarse material from valley glaciers into the lake is recorded by the >250 μ fraction of sediments, and by abundance of outsized clasts (>1cm) embedded in outcrops of the Wilson Creek Formation. Both rafting proxies were highest during early Wilson Creek time (>45 ka), reflecting the extension of long glaciers into a very deep lake. Variation of % Na_2O in the <2 μ size fraction records abundance of unaltered, clay-sized plagioclase, thought to be a measure of glacial rock flour. Covariance of magnetic susceptibility (k) and % Na_2O allows a high resolution record of rock flour contribution to the basin sediments.

Rock flour and ice-rafting proxies co-vary inversely, opposite to expectations. Possible explanations include the decoupling of flour formation by glaciers from its delivery to the lake by meltwater, or dilution of the rock flour signal by authigenic components such as sepiolite. In general, high lake level and long glaciers in early Wilson Creek time created ideal conditions for ice-rafting, followed by a lake level drop and glacier retreat. Near the end of Wilson Creek time, (<25 ka), expansion of the Tioga glaciers created large flux of rock flour, whereas rafting was low to absent due to the gap between the glacier termini and the lake shoreline.

The effect of mineral mesoporosity on amino acid adsorption

A ZIMMERMAN¹, K. GOYNE^{2,3}, J. CHOROVER²,
J. KUBICKI¹, S KOMARNENI³ AND S. BRANTLEY¹

¹ Dept. of Geosciences, The Pennsylvania State University
(azimmer@geosc.psu.edu) (kubicki@geosc.psu.edu)
(brantley@essc.psu.edu)

² Dept. of Soil, Water, and Env. Science, Univ. of Arizona
(chorover@ag.arizona.edu) (kww106@ag.arizona.edu)

³ Dept. of Crop and Soil Science, The Pennsylvania State
University (komarneni@psu.edu)

Organic matter (OM)-mineral interactions may explain diverse phenomena such as sequestration of pollutants and preservation of OM in soils and sediments. Mineral mesopores (2-50 nm diameter) have been suggested as sites of organic matter (natural and pollutant) sequestration and protection from enzymatic degradation in soils and sediments. To test this idea, we carried out batch aqueous experiments to examine adsorption of amino acid monomers and polymers onto synthetic mesoporous and nonporous alumina and silica with controlled intraparticle porosity and of similar surface chemistries.

Nearly all amino acid monomers and polymers tested exhibited significantly greater adsorption to mesoporous (8.2 nm mean pore diameter) versus nonporous alumina when normalized to surface area. Diffuse reflectance infrared Fourier transform (DRIFT) spectra show carboxylate absorption bands for sorbed glutamate and diglutamate reside at 1615 cm⁻¹ and 1570 cm⁻¹ for the nonporous and mesoporous alumina, respectively. In addition, amino acid dimers and hydrophobic monomers sorbed to mesoporous alumina exhibited adsorption-desorption hysteresis. However, a larger protein (albumin; 67 kD) adsorbed to the mesoporous alumina to a lesser extent than to the non-porous alumina. This is attributed to exclusion of albumin from the mineral mesopores where the vast majority of surface area exists. By contrast, nonporous silica adsorbed more amino acid and protein, perhaps due to the smaller pore size of mesoporous silica (3.4 nm mean pore diameter).

Adsorption of amino acids to mineral surfaces is, therefore, enhanced by mesoporosity due to stronger bond energies (perhaps bidentate versus monodentate) for organic compounds sorbed to internal versus external surfaces. Since we observe that larger macromolecules (such as enzymes and proteins) are hindered from entering mesopores, these findings provide a potential mechanism for selective sedimentary OM preservation.

Isotopic compositions of small presolar dust grains

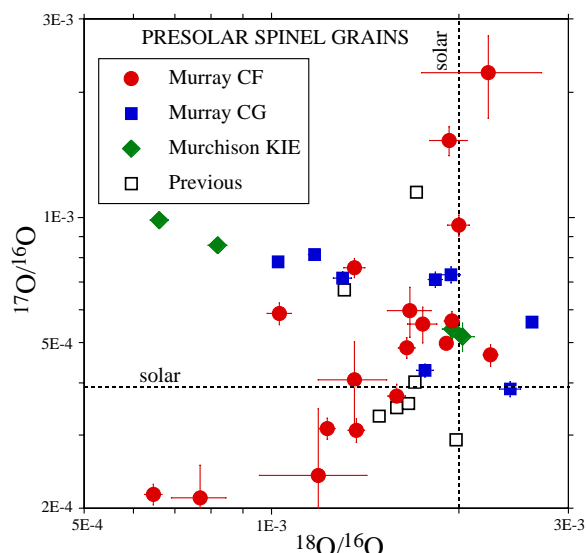
E. ZINNER, S. AMARI, R. GUINNESS, A. NGUYEN AND
F. J. STADERMANN

Laboratory for Space Sciences and the Physics Department,
Washington University, One Brookings Drive, St. Louis,
MO 63130, USA (ekz@howdy.wustl.edu)

The last ten years have seen the accumulation of a wealth of isotopic data on presolar dust grains obtained with the ion microprobe [e.g., 1]. Most of these measurements were performed on grains $\geq 1 \mu\text{m}$ in size. A new type of ion probe, the NanoSIMS, with its high sensitivity and high spatial resolution [2] offers the opportunity to analyse much smaller grains, in the size range typical for interstellar dust.

We have initiated a series of NanoSIMS presolar grain studies that exploit these new capabilities. In one example we have extended C and N isotopic measurements to much smaller SiC grains by analysing grains from Murchison separate KJB (grain diameters 0.25–0.45 μm) and Indarch IH6 (0.25–0.65 μm) [3]. The distributions of the C and N isotopic ratios are quite similar to those of larger (1.8–3.7 μm) grains from Murchison separate KJG [4, 5], the only difference being a higher fraction of grains with $10 <^{12}\text{C}/^{13}\text{C} < 40$. Indarch IH6 contains also Si₃N₄ grains and we tentatively identified some of them as presolar with isotopic characteristics similar to mainstream SiC grains.

Another study is concerned with O isotopic measurements of small spinel grains. The abundance of $>1 \mu\text{m}$ presolar spinels is very low and before the start of our study only 7 such grains had been identified. We analysed spinels from Murray CF (average size $\sim 0.15 \mu\text{m}$), Murray CG ($\sim 0.45 \mu\text{m}$) and Murchison KIE ($\sim 0.5 \mu\text{m}$) and identified 30 presolar grains (Figure 1). The abundance of presolar spinel is $\sim 3\%$ among the smallest size fraction (CF), much higher than among larger grains.



Biogeochemical cycling of C, O, and S in an iron rich hypersaline microbial mat

ZOPFI, J.¹, A. WIELAND², M. KÜHL²

¹ Danish Center for Earth System Science, Univ. Southern Denmark, Odense, Denmark (jzopfi@biology.sdu.dk)

² Marine Biological Laboratory, Univ. Copenhagen, Helsingør, Denmark (mblaw@get2net.dk), (mkuhl@zi.ku.dk)

Introduction: Although there are examples of iron rich stromatolites in the geological record, possible modern analogues have not been studied in detail as yet. We chose a cyanobacterial mat from a Solar Saltern on the Rhone Delta (Southern France) as a model system to quantify the major biogeochemical processes and to study sulfide oxidation in particular.

Approach: During a diel cycle microsensor profiles of O₂, H₂S, and pH were repeatedly measured *in situ* in the top few millimeters of the mat. At the same time the sulfate reduction rate (SRR) was determined with ³⁵S-radiotracer and mapped in 2D with ³⁵SO₄²⁻-coated silver foils. Samples for high-resolution chemical speciation (Fe(II), Fe(III), Mn(II), S⁰, S₂O₃²⁻, SO₃²⁻) were also taken. Enrichments for several sulfur- and iron-metabolizing microorganisms were established to complement the geochemical data.

Results: Microsensor profiles revealed that, unlike in other mat types, sulfide is absent in the top few millimeters even during most part of the night. However, very high SRR of up to 1800 nmol cm⁻³ h⁻¹ were determined by the ³⁵SO₄²⁻-radiotracer method. The rates were about 6 times higher during the day than the night and closely followed the diel temperature oscillations. The SRR modeled from sulfide microprofiles showed the same trend but were always much lower. During the day the difference between the gross SRR (³⁵SO₄²⁻) and net SRR (modeled) can be explained by chemical and biological oxidation of sulfide in the oxic zone and by anoxygenic phototrophic sulfide oxidation below. These processes do not operate in the dark, but measurements of Fe(II), Fe(III), and S⁰ suggest that an iron-oxide pool is built up during the day and serves as the oxidant for sulfide in the night. As a consequence, the sulfide concentrations in the top millimeters of the mat are kept low, and the SRR calculated from profiles is strongly underestimated. In the uppermost layer, S⁰ and possibly FeCO₃ are produced during the reaction of sulfide with iron oxides. FeS is formed deeper down and reaches concentrations as high as 200 μmol cm⁻³.

Conclusion: Exceptionally high iron concentrations were measured in a hypersaline microbial mat. The iron oxides in the uppermost layer of the mat act as a rechargeable sulfide buffer and as a result, sulfide oxidation gets temporally decoupled from oxygen production.

Stable Isotope analysis of volatile organic contaminants at trace levels

L. ZWANK¹, S. LUZI¹, M. BERG¹, T. C. SCHMIDT², AND S. B. HADERLEIN²

¹ Swiss Federal Institute for Environmental Science and Technology, Duebendorf, Switzerland (luc.zwank@eawag.ch)

² Center for Applied Geosciences (ZAG) Eberhard-Karls University, Tuebingen Germany

Background

Compound-specific isotope analysis (CSIA) is a very promising approach to help determining both *in-situ* transformation processes of pollutants in contaminated aquifers as well as sources of groundwater contaminants. Various laboratory studies have demonstrated the potential of this tool in contaminant hydrology (1-3). To date, the use of CSIA in field studies is, however, confined to near source zones of groundwater contamination with high pollutant concentrations. The method detection limits in CSIA are in the order of 150 ppb for chlorinated solvents using solid phase microextraction as preconcentration method (4). Hence the method sensitivity is currently too low for applications of CSIA to investigate tail and fringe zones of contaminant plumes, which would be most helpful to assess natural attenuation processes in the field.

Improvement of Sensitivity and Field Application

In order to improve the method detection limits of CSIA, we used online purge and trap (P&T) preconcentration and investigated its effects on the isotopic composition of the analytes. Evaluated parameters include purge time, desorption temperature and trap material. Isotopic fractionation effects of the various processes involved in P&T (i.e., evaporation, sorption, desorption, and condensation of the analytes) have been evaluated for a series of analytes. The effects were found to be compound-specific but showed a high reproducibility. The developed P&T-GC/IRMS method allows reproducible δ¹³C-determinations for volatile organic compounds at concentrations below 5 μg/L. P&T-GC/IRMS was successfully applied to study the fate of halogenated solvents in a contaminant plume downgradient of a municipal landfill. Contrary to previous evaluations based on concentration data alone, our P&T-GC/IRMS data strongly suggest the absence of *in-situ* degradation of trichloroethene (TCE) despite the presence of *cis*-dichloroethene, a known metabolite of (TCE).

References

- (1) Ahad, J.M. E.; Lollar, B.S.; Edwards, E.A.; Slater, G.F. and Sleep, B.E., (2000), *Environ. Sci. Technol.* **34**, 892-896.
- (2) Hunkeler, D.; Aravena, R.; Butler, B.J., (1999), *Environ. Sci. Technol.* **33**, 2733-2738.
- (3) Meckenstock, R.U.; Morasch, B.; Warthmann, R.; Schink, B.; Annweiler, E.; Michaelis, W.; and Richnow, H.H., (1999), *Environ. Microbiol.* **1**, 409-414.
- (4) Hunkeler, D. and Aravena, R., (2000) *Environ. Sci. Technol.* **34**, 2839-2844.

